



## Effect of extracellular polymeric substances on the mechanical properties of *Rhodococcus*



Yu Pen<sup>a,b</sup>, Zhenyu J. Zhang<sup>a,\*</sup>, Ana L. Morales-García<sup>a</sup>, Matthew Mears<sup>a</sup>, Drew S. Tarmey<sup>c</sup>, Robert G. Edyvean<sup>b</sup>, Steven A. Banwart<sup>d</sup>, Mark Geoghegan<sup>a</sup>

<sup>a</sup> Department of Physics and Astronomy, University of Sheffield, Sheffield S3 7RH, UK

<sup>b</sup> Department of Chemical and Biological Engineering, University of Sheffield, Sheffield S1 3JD, UK

<sup>c</sup> School of Medicine, University of Nottingham, Royal Derby Hospital, Uttoxeter Road, Derby DE22 3DT, UK

<sup>d</sup> Department of Civil and Structural Engineering, University of Sheffield, Sheffield S3 7HQ, UK

### ARTICLE INFO

#### Article history:

Received 4 August 2014

Received in revised form 1 November 2014

Accepted 6 November 2014

Available online 22 November 2014

#### Keywords:

AFM

Bacterial cell probe

Extracellular polymeric substances

Force spectroscopy

Polyelectrolytes

*Rhodococcus*

### ABSTRACT

The mechanical properties of *Rhodococcus* RC291 were measured using force spectroscopy equipped with a bacterial cell probe. Rhodococcal cells in the late growth stage of development were found to have greater adhesion to a silicon oxide surface than those in the early growth stage. This is because there are more extracellular polymeric substances (EPS) that contain nonspecific binding sites available on the cells of late growth stage. It is found that EPS in the late exponential phase are less densely bound but consist of chains able to extend further into their local environment, while the denser EPS at the late stationary phase act more to sheath the cell. Contraction and extension of the EPS could change the density of the binding sites, and therefore affect the magnitude of the adhesion force between the EPS and the silicon oxide surface. By treating rhodococcal EPS as a surface-grafted polyelectrolyte layer and using scaling theory, the interaction between EPS and a solid substrate was modelled for the cell approaching the surface which revealed that EPS possess a large capacity to store charge. Changing the pH of the surrounding medium acts to change the conformation of EPS chains.

© 2014 The Authors. Published by Elsevier B.V. This is an open access article under the CC BY license (<http://creativecommons.org/licenses/by/3.0/>).

### 1. Introduction

Oil spills and toxic compounds discharged from industrial activities and agriculture are examples of processes causing significant hydrocarbon contamination. Bioremediation is regarded as a non-destructive, cost-effective and environmentally friendly way to clean up the pollutants under circumstances which limit the viability of other remediation strategies [1]. Several members of the genus *Rhodococcus* have been widely used in bioremediation due to their ability to adapt to temperature [2,3], heavily contaminated water and soil [4,5], and radioactive environments [6]. *Rhodococci* are used to degrade xenobiotic contaminants [7], to desulphurise coal derivatives in water [8], and are involved in many engineered and in situ bioremediation processes to reduce contaminant loads in water and soil [7,9]. In addition, most *Rhodococcus* species exhibit low pathogenicity, are not eco-toxic [10], and are unlikely to generate toxins or antimicrobial compounds [11,12], indicating the utility of *Rhodococcus* species for biodegradation [13].

Extracellular polymeric substances (EPS) are crucial for cell–cell adhesion and comprise exopolysaccharides, extracellular proteins, humic substances, nucleic acids, and phospholipids [14]. There is evidence suggesting that EPS could form the framework of the biofilm matrix, determine the physicochemical properties of the biofilm [14], trap dissolved organic matter in the vicinity of the cell surface [15,16], and reduce the shear stress from water drag [17]. The physical and chemical properties of EPS at different growth stages are particularly important because the EPS determine the ability of the bacterium to trap charged contaminant colloids, adhere to substrata, and resist external forces, all of which influence the degree of bioremediation.

Efforts have been made to understand the interaction between cells and mineral surfaces, which have confirmed that the behaviour of attached cells is mediated by the physical and chemical interactions of the macromolecules at the interface [18–20]. In the present study the mechanical properties of *Rhodococcus* are modelled by considering an EPS enclosed rhodococcal cell as an analogue to a sphere with a hydrophobic core (mycolic acid covered cell wall) and a charged corona (EPS). EPS are here considered as polymers tethered to the cell surface, so that they can be treated as surface-grafted polymer chains (known as brushes, where the distance between grafting sites is shorter than the unstretched polymer end-to-end distance [21–25]). Most bacterial EPS exhibit anionic characteristics due to uronic acids (containing carboxyl

\* Corresponding author at: Department of Chemical and Process Engineering, University of Strathclyde, Glasgow G1 1XJ, UK. Tel.: +44 141 5482393; fax: +44 141 5482539.

E-mail address: [zhenyu.zhang@strath.ac.uk](mailto:zhenyu.zhang@strath.ac.uk) (Z.J. Zhang).

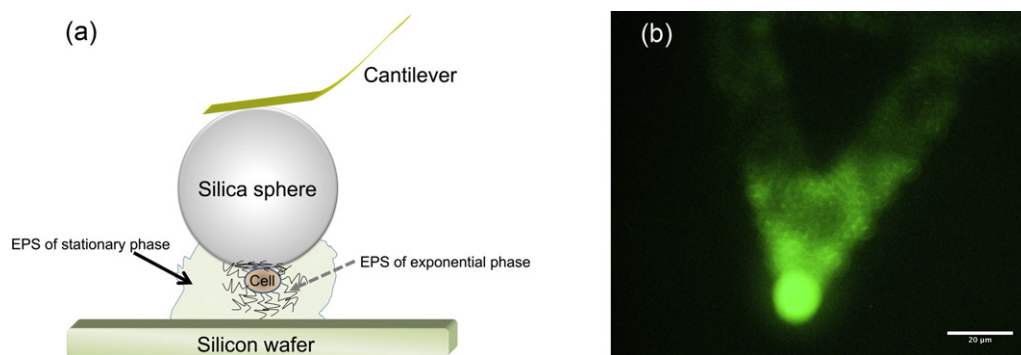


**Fig. 1.** (a) Schematic diagram of a bacterial cell probe enclosed by EPS. Cells are linked to the silica sphere via adhesive layer, but not attached to the model substrate (silicon wafer). The diagram represents an idealized view, and those cells not involved in force measurements are not shown here. (b) Fluorescence microscopy image of a cell probe that had been treated with SYTO 9 cell staining. An enhanced green colouration on the colloidal probe confirms that the particle is fully covered by rhodococcal cells.

groups), which are a major component of the exopolysaccharides [26]. It is therefore reasonable to treat EPS as weak polyelectrolytes, i.e. long chain macromolecules possessing ionizable groups [27]. This allows quantitative modelling of the repulsive force between the EPS and a solid surface when they approach each other, taking into account both electrostatic and steric forces [28]. It is worth noting that the above approach has been applied successfully not only to polyelectrolyte brushes [29,30] but also to dense layers of physisorbed homopolymers [31,32].

Initial studies of cell–surface interactions focused on the chemical structure, biological functions, and physicochemical properties of extractable EPS [33–35]. Nevertheless, measurements of interactions between extracted EPS and mineral surfaces generally ignored the contribution from non-extractable EPS and other minor components on the cell surface. The extraction process may also damage the cells, leading to the release of intracellular material and furthermore it may rupture the bonds between macromolecules, which would deform the structural integrity of the EPS. Unlike experiments using only extracted EPS, a bacterial cell probe as shown in Fig. 1 offers the opportunity to measure cell–mineral interactions under biological conditions. Several studies have been carried out to investigate steric interactions, adhesion, and viscoelasticity of the EPS of different bacterial strains [24, 36–40], but few have examined the contribution of EPS to the mechanical properties of whole cell. Bacterial cell probes made of cells chosen at different growth stages enable the characterization of the mechanical properties of *Rhodococcus* as a function of growth stage, which are important parameters in understanding its effectiveness in bioremediation.

Atomic force microscopy (AFM) can be used to measure forces between a sample surface and a fabricated probe (tip) attached to the apex of a cantilever, and measurements can be performed in liquids analogous to the natural biological environment. Force spectroscopy, a variant of AFM, measures the interaction as a function of probe-sample distance in the normal direction [41]. By attaching cells from different growth stages to the AFM cantilever, the mechanical properties of *Rhodococcus* are studied in terms of their: (1) charge storage, (2) water retention capability, and (3) adhesion to a model surface.

## 2. Materials and methods

### 2.1. Cultivation of *Rhodococcus*

*Rhodococcus* RC291, isolated from a contaminated gas-works site in the North East England [42], was kindly donated by J. A. C. Archer (University of Cambridge). Rhodococcal cells from a  $-70^{\circ}\text{C}$  glycerol stored stock were spread on a Petri dish containing sterile solid Luria-Bertani (LB) agar (Fisher Scientific) using a sterile loop (1 mL). Thereafter, the Petri dish was kept in an incubator at  $25^{\circ}\text{C}$  (TSE 33644, Sanyo) for 36 h and then refrigerated at  $4^{\circ}\text{C}$  ready for use. A liquid LB medium

(Fisher Scientific) (20 g/L) was prepared using de-ionized (DI) water (Elga PURElab option,  $18\text{ M}\Omega\cdot\text{cm}$ ) prior to being sterilized in an autoclave at  $121^{\circ}\text{C}$  for 20 min. Glucose solution (2 mM) was autoclaved separately.

A colony of *Rhodococcus* sp. RC291 was taken from the solid agar medium using a sterile loop (1 mL) and then inoculated into the LB liquid medium (100 mL) together with glucose (2 mM) in a pre-sterilized flask (300 mL). The flask was then placed on an orbital rotary shaker (DOS-20 L, ELMi Ltd.) at 150 rpm in an incubator at  $25^{\circ}\text{C}$  for 6 h (late exponential phase), 24 h (mid-stationary phase), or 36 h (late stationary phase) based upon the growth curve shown in Fig. 2. The cell concentration was expressed in terms of optical density measured by spectrophotometry (S2100 UV/Vis Diodo Array Spectrophotometer, Biochrom, Biowave WPA).

### 2.2. Preparation of bacterial cell probe

1 mL of rhodococcal cells in LB liquid medium were transferred to a centrifuge tube (1 mL), and then centrifuged at  $12,100\text{ g}_n$  (where  $\text{g}_n$  is the standard acceleration due to gravity) for 2 min, as suggested by previous studies [43–45]. (At this acceleration, only weakly bound EPS are removed as described below.) The presence of a cell pellet was confirmed after centrifugation. 0.95 mL of supernatant was removed and replaced by phosphate buffered saline (PBS: 0.2 g/L KCl, 8 g/L NaCl, 1.44 g/L  $\text{Na}_2\text{HPO}_4$ , and 0.24 g/L  $\text{KH}_2\text{PO}_4$  at pH 7.4) [46], and vortexed to mix [47]. The PBS washing procedure was repeated three times to wash away cell debris and liquid medium remaining on the cell surfaces to enhance cell attachment onto the AFM cantilever. Cells were washed three more times using DI water prior to being concentrated. Fluorescence microscopy was used to confirm that the preparation procedure does not damage the cells.

To prepare a bacterial cell probe, a  $10\text{ }\mu\text{m}$  diameter silica sphere (Duke Scientific, USA) was attached to the apex of an AFM cantilever (MLCT, Bruker probes) using epoxy glue. The colloidal probe was then immersed in 5 wt% poly(D-lysine) (weight average molecular mass 4000 g/mol) solution for 15 s to functionalize, and then exposed in air for 15 min. Poly(D-lysine) is a polycation used to bind a negatively charged cell surface through its amino groups [48,49]. The poly(D-lysine) functionalized colloidal probe was immersed in a drop of the concentrated cell solution ( $5\text{ }\mu\text{L}$ ,  $\sim 10^9$  cell/mL), and both were then exposed in air for 40 min. Thereafter, the probe was rinsed with DI water to remove unattached cells. The comparable sizes of a silica particle ( $10\text{ }\mu\text{m}$  in diameter) and a rhodococcal cell (of length  $\sim 2\text{ }\mu\text{m}$ ) ensure that only one cell is measured during the experiment. A schematic diagram of an idealized bacterial cell probe enclosed by EPS is shown in Fig. 1a.

Cell staining was necessary to verify the existence of cells on the colloidal probe, and more importantly, whether the cells remain viable/active. Control experiments, applying a green-fluorescent nucleic acid

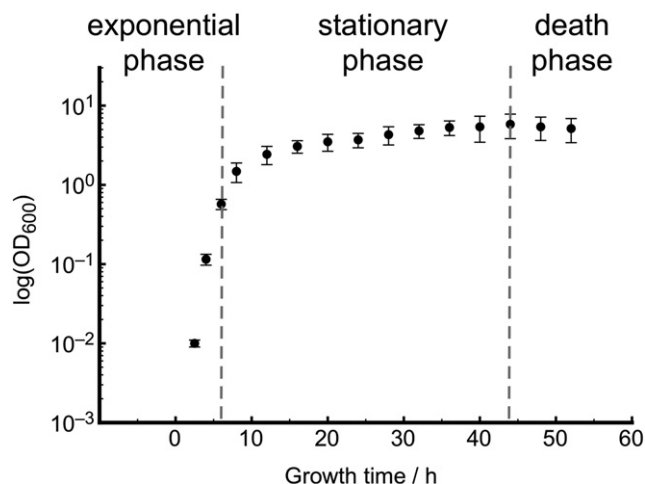


**Fig. 2.** Growth profile of *Rhodococcus* sp. RC291 in a LB + glucose (2 mM) medium on a shaker (150 rpm) at 25 °C. The cells were collected after incubation for 6 and 36 h. The cell concentration was expressed in terms of optical density ( $OD_{600}$ ) measured by spectrophotometry at a wavelength of 600 nm.

stain (LIVE/DEAD BaLight, Molecular Probes) to the cells, were performed before and after force measurements. For fluorescence microscopy, an Olympus BX51 microscope equipped with a WIBA filter cube (excitation filter, 460–490 nm band pass; barrier filter, 510–550 nm band pass) was employed. A typical cell probe treated with SYTO 9 is presented in Fig. 1b, which shows a great number of cells were attached to the probe. Therefore, the force curves recorded in the experiments were confirmed as cell–silicon interactions instead of silicon–silicon or poly(D-lysine)–silicon interactions.

### 2.3. Contact angle measurements

To examine the effect of the washing procedure on the surface properties of cells, rhodococcal cells incubated for 6, 24, and 36 h were concentrated at 1200  $g_n$  for 10 min. The pellets were then resuspended in PBS, separated in groups A, B and C, and every group was washed by the corresponding protocol: (A) 7 times in 1 mL PBS; (B) 3 times in 1 mL PBS, then 3 times in 1 mL DI water, followed by 1 time in 1 mL PBS; and (C) 3 times in 1 mL PBS, then 3 times in 1 mL DI water. Centrifugation at 12,100  $g_n$  was performed for 2 min in each cycle. The cells were then filtered using a Millipore glass microanalysis filter holder with fritted glass; a vacuum pump, and Isopore polycarbonate membrane filters (0.2  $\mu$ m, GTTP, Merck Millipore, USA). Vacuum was applied until the bacterial lawns were reasonably dry. The filters were left to dry further inside Petri dishes with filter paper bottoms for 30 min. Contact angle measurements were accomplished with the static sessile method using DI water (Elga PURElab option, 18 M $\Omega$ ·cm) and measured with an optical tensiometer (Attension, Biolin Scientific, Espoo, Finland). Surface tensions were calculated using the built-in software by averaging over 300 frames of contact angle.

### 2.4. Preparation of model substrates

Silicon wafers (Prolog Semicor Ltd., Ukraine) were cut into 1 × 1 cm<sup>2</sup> pieces and immersed in RCA-1 solution (pure water, ammonia solution, and hydrogen peroxide with a volume ratio 5:1:1) at 75 °C for 15 min to remove organic contaminants. The silicon pieces were then rinsed with copious DI water, and dried under nitrogen. The substrates were cleaned by oxygen plasma for 15 min shortly before the experiments.

### 2.5. Force spectroscopy

Concentrated hydrogen chloride or sodium hydroxide solution was added to DI water to prepare solutions of pH 3.0 and 10.0. DI water exposed in air for 30 min possessed a pH of 6.5. Sodium chloride was then added to the aqueous solutions of different pH at concentration of 1 mM. A molecular force probe (MFP 1D, Asylum Research, CA, USA) was employed for force measurements. The force measurements were carried out in liquid by submerging the cell probe in the aqueous medium at 25 °C. The spring constant of the AFM cantilever was calibrated in the same solution before cells were attached using the built-in thermal fluctuation method [50]. The approach speed of the probe was 1  $\mu$ m/s and the pulling distance was 5  $\mu$ m with no dwell time allowed for the probe on the substrate. The start distance was automatically synchronized according to the approach speed and the pull distance. The applied force was kept at 10 nN throughout the measurements. Over 500 force curves were collected during each measurement. Force spectroscopy experiments were repeated at least three times in each condition using freshly prepared bacterial cell probes. Adhesion between a poly(D-lysine) covered probe and a silicon oxide surface in the same pH range was measured as control experiments.

### 2.6. Determination of contact point, cell spring constant and EPS thickness

A soft probe (in the present study, a cell covered by EPS layer) deforms when it is compressed by a rigid surface, which makes it difficult to define the exact contact point. Here the onset of the linear compliance of the approach curve is defined as the contact point; it is convenient to discuss contact as the point at which the cell is mechanically perturbed, which is an arbitrary definition, convenient for the present work. Thus, the approach curve was shifted along the abscissa (Fig. 3) so that the onset of the linear compliance was at  $x = 0$  (contact point) [36,51–53].

The cell spring constants ( $k_c$ , N/m) that describe the elasticity of the cell probes, were determined by combining the cantilever spring constant ( $k_s$ , N/m) and the slope ( $S$ , N/m) of the linear compliance region ( $x < 0$ ) of the approach part of the force curve of the cell probe during the first approach using [54]

$$k_c = \frac{-Sk_s}{S + k_s} \quad (1)$$

As shown in Fig. 3, the thickness of EPS was determined by the distance ( $\Delta x$ ) between the onset of the linear compliance (the contact

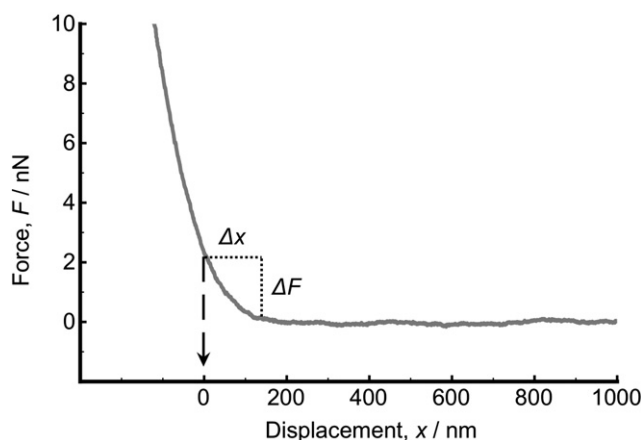


**Fig. 3.** A typical approach part of a force curve acquired on a silicon oxide surface using a biological cell probe, from which the contact point and the EPS thickness were determined. The contact point (zero distance) was defined as the onset of the linear compliance of the approach part of the force curve; the EPS thickness was determined by the distance between the contact point and the onset of the repulsion.

point) and the onset of repulsion (the outermost boundary of EPS by taking the repulsion force greater than 0.05 nN into account) on the approach curve.

### 2.7. Evaluation of grafting density, brush thickness, charge density, and differential capacitance

EPS of *Rhodococcus* were treated as polyelectrolyte brushes grafted onto the bacterial cell wall. A scaling theory is used whereby the surface consists of a fairly dense array of polyelectrolytes is end-grafted. The assumption that the EPS are end-grafted is made in order to simplify the consideration of this hitherto complex material. The analysis performed in this work demonstrates that this brush assumption yields reasonable results. The repulsive electrosteric force,  $F$ , between a spherical surface covered with charged polymer chains and a planar surface as a function of distance,  $x$ , by neglecting chain stiffening and excluded volume effects is described by [25,55]

$$F = \frac{4\pi R k_B T f N}{d^2} \ln\left(\frac{L_0}{x}\right), \quad (2)$$

where  $R$  is the radius of the rhodococcal cell,  $k_B T$  is the thermal energy,  $f$  is the monomer fraction of ionization,  $N$  is the number of monomer units per chain,  $\Gamma = 1/d^2$  is the grafting density, and  $L_0$  is the thickness of EPS. A prefactor of 2 was placed in front of  $L_0$  in a previous study [23] to account for repulsive interactions contributing equally from two surfaces bearing polymers, but it is missing here because only one surface is covered by polyelectrolytes in the present work. (There are other factors such as the existence of an electric double layer on the silicon oxide surface, or the distribution of charges across the EPS layer, which could affect the electrosteric interaction.)

The areal charge density,  $\sigma$ , can be obtained from

$$\sigma = f N e, \quad (3)$$

where  $e$  is the elementary charge.

The fraction of ionized monomers ( $f$ ) of EPS varies depending upon the pH of the solution. At a low salt concentration, in what is referred to as the osmotic brush regime, the counter-ions are trapped within the brush in a range known as the Gouy–Chapman length ( $\lambda_{GC}$ ) which is much less than the brush thickness ( $L_0$ ) [56]. Charges and (counter-) ions trapped within  $\lambda_{GC}$  from a charged surface form a diffuse electrical double layer, which can be treated as a capacitor with a simplified view because it is capable of storing electric charge. Capacitance is used as an indicator to reveal the capability of the EPS to store charge. The areal differential capacitance of the electric double layer ( $C_{GC}^A$ ) is expressed as [57],

$$C_{GC}^A = \frac{\epsilon_r \epsilon_0}{\lambda_{GC}}, \quad (4)$$

where  $\epsilon_r$  is the relative permittivity of the medium,  $\epsilon_0$  is the electric constant, and  $\lambda_{GC}$  can be expressed as [55],

$$\lambda_{GC} = \frac{1}{2\pi l_B f N \Gamma}, \quad (5)$$

where  $l_B$  is the Bjerrum length (the distance at which  $k_B T$  is equal to the Coulombic repulsion between like charges in a medium of permittivity  $\epsilon_r \epsilon_0$ ).

## 3. Results and discussion

### 3.1. Rhodococcal cell surface properties

Surface properties of microbial cells are vital to their behaviour at solid–liquid interfaces. The importance of preparation procedures such

as centrifugal speed and washing buffer used has been quantitatively confirmed in the previous work [45]. To test the validity of the preparation procedure of bacterial cell probes, the surface hydrophobicity of rhodococcal cells treated with three different washing protocols has been compared.

Contact angle results (Fig. 4) show that the hydrophobicity of cells incubated for 24 and 36 h is largely unaffected by the washing procedures, which indicates that the membrane and EPS have adequate time to form a robust hydrophilic matrix to protect the cells. However, the cells of culture time 6 h show a different response to washing processes. The sample that was treated with protocol (A): 7 rinses in 1 mL PBS shows a similar trend to that with protocol (B): 3 rinses in 1 mL PBS, then 3 times in 1 mL DI water, followed by another in 1 mL PBS, whereas those treated with 3 rinses in 1 mL PBS, followed by 3 rinses in 1 mL DI water (protocol C), are more hydrophobic. A comparison between the three sets of data indicates that cells at the mid-stationary and late-stationary phases remain largely intact after high speed centrifugation and re-suspension in water, whereas late-exponential cells have a weaker attachment to their EPS and are more likely to be separated by re-suspension in water, but not due to centrifugal speeds alone. Since rhodococcal cells are hydrophobic in nature and EPS tend to have a hydrophilic character, the loss of EPS could lead to an increase in hydrophobicity and an associated increase in the contact angle. The conformation of EPS when exposed to DI water could be different to that in PBS buffer, which causes the discrepancy observed in this study. Nevertheless, protocols (A) and (B) terminate with washing in PBS, which could leave salts on the cell surface, accounting for the smaller contact angles. Furthermore, fluorescence images (Fig. S2) of cells incubated for 24 h followed by the washing protocols confirm that the cells are alive and have EPS associated despite the washing treatment.

### 3.2. Cell spring constants, EPS expansion and shrinkage

The determination of cell spring constants was based on Eq. (1). For the cells of the late exponential phase (6 h incubation), the cell spring constants were 0.056, 0.034 and 0.026 N/m at pH 3.0, 6.5 and 10.0, respectively (Table 1), indicating that the cell was stiffer at low pH and softer at high pH. The ranges of repulsion ( $\Delta x$ ) were 0.24, 0.48 and 0.75  $\mu\text{m}$  at pH 3.0, 6.5 and 10.0, respectively. An increase of the repulsion range with increasing pH implies that the EPS swelled when the environment changed from acidic to alkaline. The negative charge on the

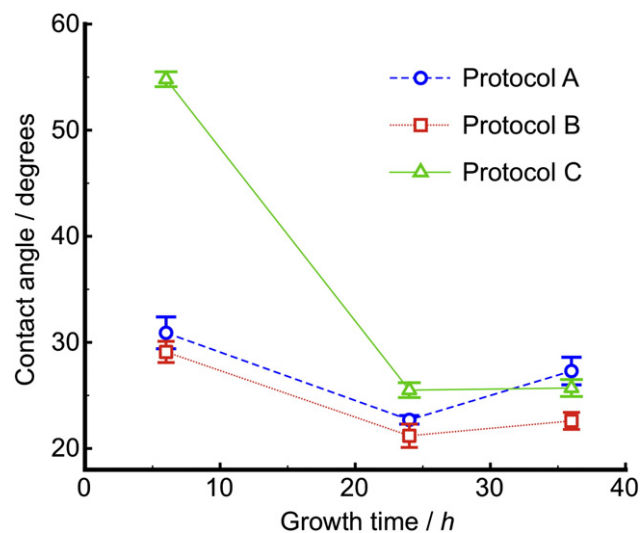


Fig. 4. Contact angle of rhodococcal cells treated with three different washing protocols: (A) 7 times in 1 mL PBS; (B) 3 times in 1 mL PBS, then 3 times in 1 mL DI water, and then once in 1 mL PBS; (C) 3 times in 1 mL PBS, then 3 times in 1 mL DI water, as a function of growth time.

**Table 1**

Cell spring constant  $k_c$  and thickness  $t_{\text{eps}}$  of the EPS of different growth stages in 1 mM NaCl solution determined by Eq. (1) and the repulsion distance, respectively. The errors represent the standard errors of the means of twenty force curves.

pH	3.0	6.5	10.0
<i>EPS – exponential phase</i>			
$k_c$ (N/m)	0.056	0.034	0.026
$t_{\text{eps}}$ ( $\mu\text{m}$ )	$0.24 \pm 0.02$	$0.48 \pm 0.03$	$0.75 \pm 0.04$
<i>EPS – stationary phase</i>			
$k_c$ (N/m)	0.043	0.026	0.024
$t_{\text{eps}}$ ( $\mu\text{m}$ )	$0.37 \pm 0.04$	$0.76 \pm 0.10$	$1.0 \pm 0.1$

silicon oxide surface at high pH should also contribute to this pH-dependent repulsion distance. For cells of the late stationary phase (36 h incubation), the cell spring constants at pH 3.0, 6.5 and 10.0 were 0.043, 0.026 and 0.024 N/m, respectively, showing that these cells also became softer as pH increased. The repulsion ranges at pH 3.0, 6.5 and 10.0 were 0.37, 0.76 and 1.0  $\mu\text{m}$ , respectively (Table 1), enlarging when increasing pH. The cell spring constants were consistent with reported values [25] being in the range 0.01–0.5 N/m, despite the cells being covered with a dense EPS layer at the late stationary phase.

### 3.3. Mechanical properties of rhodococcal cell under compression

The mechanical properties of EPS depend upon their water content: compressions apply normal stress on the EPS, and so affect water retention. Mechanical properties were examined in 1 mM NaCl solution at pH 10.0 where EPS were expected to be fully stretched. As the cell approaches the silicon oxide surface, water is expelled from the EPS whereas retracting the cell results in the reabsorption of water. For cells of the late exponential phase, the approach curves drastically shift inward after the first compression, indicating a reduced repulsion, and then remain constant during subsequent compressions (Fig. 5a), which suggests that water was removed after the first compression, and the EPS were not restored to their original state. A comparison of the approach curves of rhodococcal cells of the exponential phase at pH 3.0 and 10.0 (Fig. 5a) reveals that the repulsion (after the first compression) at pH 10.0 is greater than that at pH 3.0, which means that water content in EPS of cells at the late exponential phase at pH 10.0 is greater than that at pH 3.0.

For the rhodococcal cells of the late stationary stage, the approach curves shift slightly inward during subsequent compressions (Fig. 5b), revealing that, although compressions cause a slight reduction of water content, EPS incubated for a longer period possess stronger water retention than those of the early growth phase. A comparison of approach curves of cells of the late stationary phase at different pH (Fig. 5b) confirms that the EPS could accommodate more water at pH 10.0 than at pH 3.0.

### 3.4. Electrosteric forces between rhodococcal cell and a silicon oxide substrate

Approach curves were recorded when a bacterial cell probe was approaching the silicon oxide surface. Repulsions occurred between the cell of the late exponential phase and silicon at pH 3.0, 6.5 and 10.0 in 1 mM NaCl solution and the repulsion increased with increasing pH (Fig. 6a). Electrosteric forces are expected to govern the interactions between the cell and the silicon oxide surface. Due to the initial displacement of water in the EPS under external compression, as shown in the previous section, it is appropriate to use the very first approach curve collected to describe the electrosteric forces between rhodococcal cell and solid substrate. Fitting the force curves based on Pincus theory (Eq. (2)) suggests that the thickness of the EPS increased from 305 nm to 579 nm, while the number of charges per chain ( $fN$ ) increased from 7.0 to 12.6 when the pH of the surrounding medium increased from 3.0

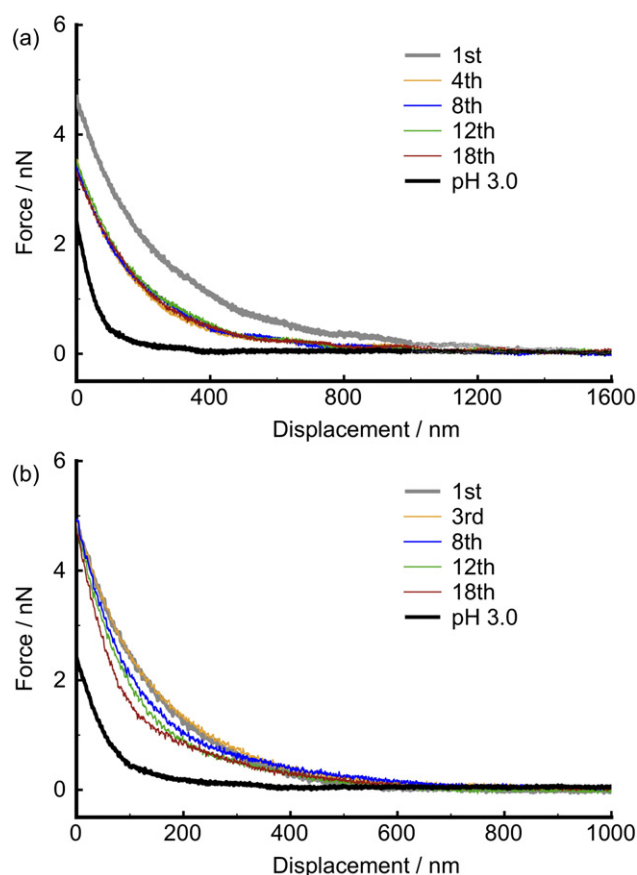


**Fig. 5.** Approach curves of an EPS-covered rhodococcal cell probe incubated for (a) 6 h and (b) 36 h against a silicon oxide surface in 1 mM NaCl solution at pH 10.0 with the number of compression cycles. For EPS of the exponential phase, the approach curves during the 1st, 4th, 8th, 12th and 18th compression are presented; for EPS of the stationary phase, the approach curves during the 1st, 3rd, 8th, 12th and 18th compressions are presented. The compressed statuses of both EPS at pH 10.0 are compared with those at pH 3.0.

to 10.0 (Table 2). As the number of monomer units ( $N$ ) of EPS chains is independent of pH, the variation of charges per chain is attributed to changes in  $f$ , the fractional ionization. The fitted grafting density of EPS chains ( $\Gamma$ ) was found constant throughout the pH range at  $1.95 \times 10^{-3}$  molecules/ $\text{nm}^2$ . The surface charge densities ( $\sigma$ ) of the rhodococcal cells at the late exponential phase can be obtained through Eq. (3) and were  $(1.45 \pm 0.01)$ ,  $(2.51 \pm 0.01)$ , and  $(2.61 \pm 0.01)$   $\text{mC} \cdot \text{m}^{-2}$  at pH 3.0, 6.5, and 10.0, respectively.

Repulsion was also observed between the cells of the late stationary phase and silicon oxide at pH 3.0, 6.5 and 10.0 in 1 mM NaCl solution, and the repulsion increased with increasing pH (Fig. 6b). Fitting the first approach curves acquired using Eq. (2) indicates that the thickness of the EPS increased from 171 nm to 489 nm when pH increased from 3.0 to 10.0, while the charge per chain increased from 12.4 to 22.0 (Table 2). Again, the grafting density ( $\Gamma = 1.34 \times 10^{-3}$  molecules/ $\text{nm}^2$ ) was found consistent from pH 3.0 to pH 10.0. The surface charge densities ( $\sigma$ ) of the rhodococcal cell obtained through Eq. (3) were  $(2.66 \pm 0.01)$ ,  $(4.29 \pm 0.01)$ , and  $(4.72 \pm 0.01)$   $\text{mC} \cdot \text{m}^{-2}$  at pH 3.0, 6.5 and 10.0, respectively. Grafting density, brush thickness, and charge density estimated based on Pincus theory are summarized in Table 2 for the EPS at different growth phases. After accounting for the effect of grafting density EPS of the stationary phase therefore have a greater capacity to store charge (Eq. (4)) than EPS of the exponential phase in the corresponding electrical double layer.

Fitting the approach curves shows that the surface charge density and thickness of both EPS increased with increasing pH, as expected for weak polyanions. The grafting density of EPS at the late exponential phase is greater than that of EPS at the late stationary phase which

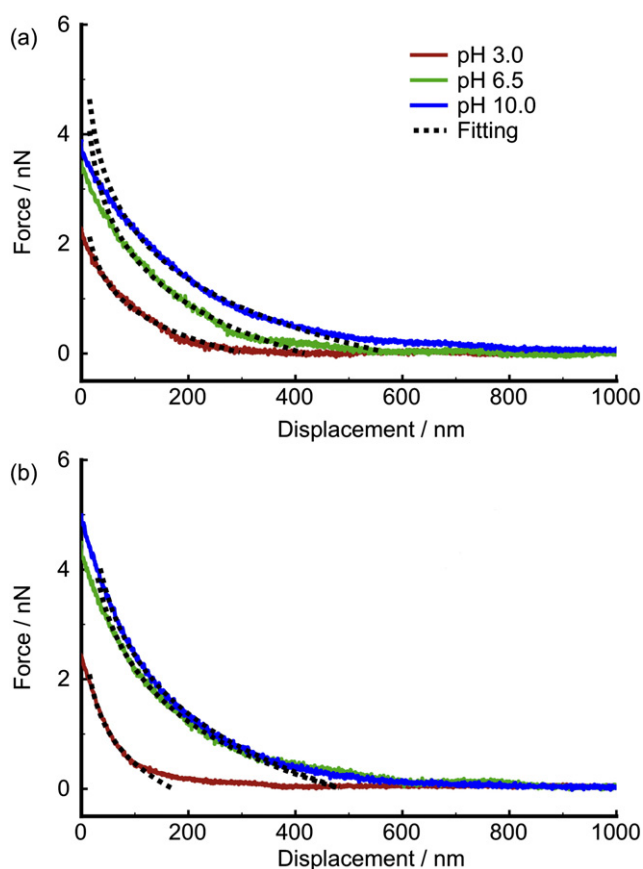


**Fig. 6.** Approach curves show repulsion between (a) EPS of the exponential phase, and (b) EPS of the stationary phase and a silicon oxide surface in 1 mM NaCl solutions at pH 3.0, 6.5 and 10.0 fitted by Pincus theory. The broken lines are the fits to the data. Variations between force curves during each experiment are negligible and therefore only the representative curves are shown here for clarity.

demonstrates the difference between the two; EPS at the late stationary phase are less densely bound but consist of chains able to extend further into their local environment, while the denser EPS at the late exponential phase act more to sheathe the cell. The estimated thickness of EPS at the late exponential phase and the late stationary phase (at pH 10.0) are 579 and 489 nm, respectively. These values are much greater than the distances between grafting sites ( $d$ ) (22.6 and 27.3 nm for the exponential and the stationary phase EPS, respectively), indicating that the assumption of considering EPS as surface grafted brushes is valid.

Even though a large repulsion of few hundred nanometres was observed for cells of a different growth stage, this is not unusual as the same magnitude of repulsion was reported in previous works. For example, long range repulsion was found when standard AFM tip was used to compress the surface-immobilized *Escherichia coli* [39]. Similar long range repulsion has also been reported in a separate study where *Pseudomonas putida* was studied in 1 mM MOPS buffer [24]. In that

**Table 2**

Grafting density ( $\Gamma$ ) thickness ( $L_0$ ), and number of charges per chain ( $fN$ ) of the EPS in 1 mM NaCl solution determined from Pincus theory.

pH	3.0	6.5	10.0
<i>EPS – exponential phase</i>			
$\Gamma$ ( $\times 10^{-3}$ nm $^{-2}$ )	1.95	1.95	1.95
$L_0$ (nm)	305 $\pm$ 3	418 $\pm$ 3	579 $\pm$ 2
$fN$	7.0 $\pm$ 0.1	12.1 $\pm$ 0.1	12.6 $\pm$ 0.04
<i>EPS – stationary phase</i>			
$\Gamma$ ( $\times 10^{-3}$ nm $^{-2}$ )	1.34	1.34	1.34
$L_0$ (nm)	171 $\pm$ 2	486 $\pm$ 2	489 $\pm$ 1
$fN$	12.4 $\pm$ 0.1	20.0 $\pm$ 0.1	22.0 $\pm$ 0.1

work, the equilibrium length of bacterial surface polymer was found to increase from 230 to 750 as solution pH increases from 4.75 to 8.67. Such a trend is in good agreement with the present work where EPS take an extended conformation at high pH due to its nature negatively charge.

### 3.5. Adhesion of rhodococcal cell to a silicon oxide surface

The adhesion force between EPS and silicon oxide was determined by the maximum force of retraction curves. For EPS of cells incubated for 6 h (Fig. 7a), the adhesion force, shown as the minimum in the retraction curves, was 1.9 nN at pH 3.0, whereas no adhesion but hysteresis was observed at pH 6.5 and 10.0. The apparent adhesion peaks could only be detected at pH 3.0 and are attributed to the condensation of counter-ions in the EPS during compression, which results in the formation of hydrogen bonds between EPS and the silicon oxide surface at low pH [58]. The adhesion energy was calculated from the area enclosed by the approach (not shown in Fig. 7) and the retraction parts, and averaged over 200 force curves. The adhesion energy ( $\sim 8 \times 10^{-16}$  J) was found to be independent of pH, even though no adhesion peak was observed for high pH.

Although the conformation of EPS on solid substrates changes as a function of pH, the adhesion energy is not a basic thermodynamic property, therefore the independence of adhesion energy with pH is likely to be due to two different effects competing against each other. From the data in Fig. 6a for EPS of the exponential stage compressed at a different pH level, it was found that the EPS are more extended at higher pH, which indicates a larger contact area formed between bacterium and solid substrate (even though this cannot be quantified). In the present work, adhesive interactions between the EPS and the surface are greater at low pH than at high pH, where there are no clear or visible

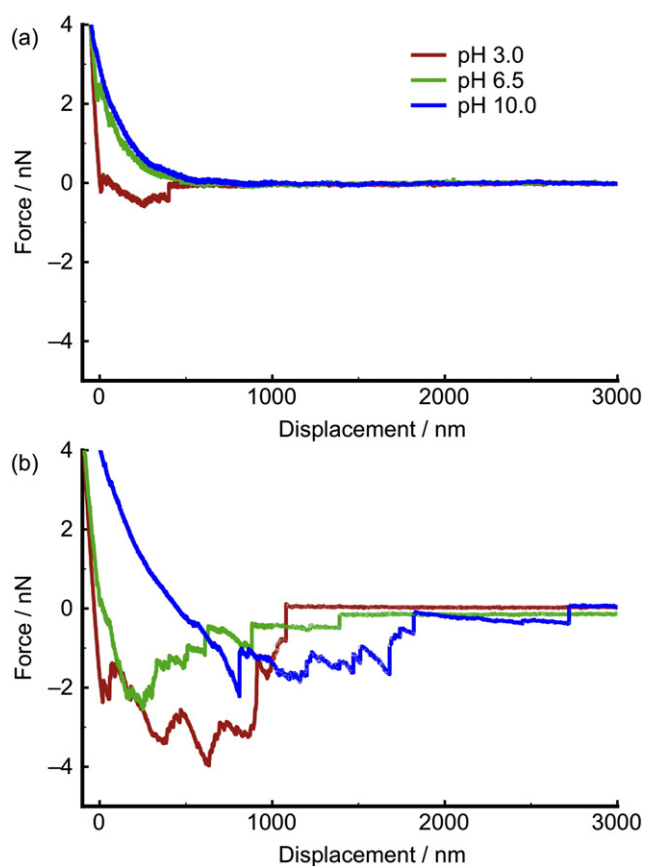


**Fig. 7.** Adhesion (retraction part of the force curves) between an EPS-covered rhodococcal cell probe incubated for (a) 6 h and (b) 36 h and a silicon oxide surface in 1 mM NaCl solutions of different pH.

interactions at all (Fig. 7a). It is therefore believed that the large adhesion force at pH 3, combined with a small contact area will result in an adhesion energy of the same magnitude that is generated by weaker adhesion force with larger contact area at pH 10.

It is worth noting that the retraction part of the force curves of EPS incubated for 36 h, as shown in Fig. 7b, exhibits saw-tooth patterns, indicating the extension and rupture of multiple bonds when the cell probe was being retracted from the silicon surface. For rhodococcal cells of the late stationary phase adhesion was observed at all pH. The maximum stretching distance, which also can be defined as the adhesion distance, increases by increasing the pH of the surrounding medium in agreement with the fitting results that EPS take the most extended conformation at high pH. The magnitude of the adhesion decreases from low to high pH suggesting a reduced attraction between rhodococcal cells incubated for 36 h and the silicon oxide. However, as for EPS of the late exponential phase, the adhesion energy ( $\sim 3.2 \times 10^{-15}$  J) was found to be constant for all pH.

The range of adhesion forces for microbial attachment to porous media measured by AFM has been summarized in a recent review [59]. The magnitude of the adhesion force measured in the present work falls within this range.

### 3.6. General discussion

In the rhodococcal cell envelope, the space spanned by lipoglycans, which are members of the lipoarabinomannan (LAM) family [60–62], anchored between the outer leaflet of the cytoplasmic membrane and the peptidoglycan layer, is regarded as a pseudo-periplasm [63]. Carboxyl and phosphate groups in the LAM layer have been found in mycobacteria [64]. Peptidoglycan, a crosslinking polymer through a 1,4- $\beta$ -linkage between *N*-acetylglucosamine and *N*-acetylmuramic acid [37], is considered to contribute to the negatively charged properties of the cell wall [65,66]. When the cell probe approached the silicon oxide substrate, it is likely that the linear compliance region of the force curves was induced by progressively compressing the pseudo-periplasm and the cytoplasmic membrane maintained by turgor pressure [67]. The enlargement in the pseudo-periplasm and the increase of water content in EPS result in a change of cell spring constants [67–69]. A comparatively greater spring constant of the EPS at the early growth stage than that of the EPS incubated for 36 h at all pH indicates that the latter are capable of accommodating more water, assuming the enlargements in the pseudo-periplasm of the cell enclosed by both EPS are the same.

The thickness of EPS is pH responsive due to them being weak polyelectrolytes. Carboxylate and phosphate are functional groups that give anionic characteristics to EPS. Alkaline environments deprotonate carboxyl groups and cause repulsion among the EPS brushes, thereby stretching the EPS. Determining the thickness of the EPS layer is challenging in the present study since the EPS are easily deformed; the thickness was defined based on the repulsion distance, or estimated by fitting the approach curves with Pincus theory. For EPS of the late stationary phase, significant deviations were found between the values determined by using the above methods, particularly at high pH, although the values are close for the EPS of the late exponential phase. This is because the thickness of the EPS incubated for 36 h is determined from the repulsion distance, which includes the thickness of the EPS of the late exponential phase, which is not considered in the application of Pincus theory in the present work.

Deviations of the experimental data from Pincus theory were observed and can be ascribed to the following effects:

- The cell shape is elliptic instead of spherical, leading to a deviation from Pincus theory which requires the interaction is between a sphere and a planar surface.
- The repulsion at the onset of the approach curves is due to the steric force; Pincus theory considers electrosteric interactions, which are only effective over a range of  $\lambda_{GC}$ .

- Weak polyelectrolyte brushes do not necessarily exhibit a uniform monomer concentration profile assumed by Pincus theory in the osmotic brush regime [70,71], which could cause a deviation of the Pincus theory predictions from the experimental results, especially at high pH where the EPS chains are stretched.

In the compression measurements, water could be easily forced out of the EPS of the exponential phase because they are relatively less ionic than those of stationary phase; hence water molecules do not bind strongly to the EPS. It was found that EPS of the stationary phase exhibit better resistance against compression than EPS of the exponential phase, which is likely to be due to the better water retention of the EPS of the former. Water retained in EPS incubated for 36 h enhances the robustness of the EPS, thereby protecting the enclosed cells. Slight shifts in the approach curves after continuous compressions indicate little water loss, and EPS of cells incubated for 36 h are more resilient to normal stress than those incubated for 6 h. Rhodococcal polysaccharides, which are present in both the exponential and the stationary phase contain rhamnose, galactose, glucose, and glucuronic acid [72], of which rhamnose is considered to be the least water-soluble.

The EPS of rhodococcal cells at the stationary phase are regarded as amorphous random coils probably due to the 1,2- $\alpha$ - or 1,6- $\alpha$ -linkages between their exopolysaccharides. The presence of acyl substitutes (e.g. O-acetyl groups) helps the EPS incubated for 36 h to form an ordered helical architecture [73] so as to resist normal compression. The EPS of the late exponential phase, nevertheless, may possess 1,3- $\beta$ - or 1,4- $\beta$ -linkages between the exopolysaccharides [73] resulting in rigid helices that are less resilient to normal compression.

Most bacterial EPS comprise anionic polysaccharides with a minor portion of proteins and hydrophobic residues [74,75]. Active sites in the EPS are composed of functional groups such as amine, carboxyl, hydroxyl, and phosphate groups. These sites could promote the affinities of EPS to ions, dissolved organic molecules (including amino acids, peptides, and proteins), and organic colloids [76,77]. Significant adhesion forces were measured between EPS of the late stationary phase and silicon oxide surface at all pH, whereas little adhesion was observed between EPS of the late exponential phase and silicon oxide surfaces except at pH 3.0. Such differences indicate that most binding sites available to interact with the silicon oxide are located in the EPS incubated for 36 h. Although the EPS of the exponential phase account for initial cell attachment before the EPS of the stationary stage are excreted, data in the present study confirm that EPS at the late growth stage play a crucial role in cell adhesion and aggregation [78]. When changing the pH of the aqueous medium, the density of those binding sites varies in accordance with the conformation of the EPS chains. At pH 3.0, the magnitude of the adhesion between EPS incubated for 36 h and the silicon oxide surface is the largest while the adhesion distance is the shortest. This is because EPS chains take a collapsed (or contracted) conformation at pH 3.0 so that a short range of interaction is expected, whereas at pH 10.0 EPS chains take an extended conformation resulting in fewer binding sites per unit volume and have an influence over significantly longer distances. The adhesion energy between EPS of the rhodococcal cell at the late stationary phase and the silicon oxide surface was found to be consistent throughout the pH range studied. Adhesion between the EPS incubated for 36 h and the silicon oxide surface is most likely to be due to these non-specific binding sites and that the number of the non-specific binding sites in the EPS of the late growth stage does not change. Furthermore, while changes in pH do not affect the number of the binding sites, they do affect the density of the binding sites.

## 4. Conclusion

By carrying out force measurements using a cell-functionalized probe, the interaction between an EPS covered rhodococcal cell and a model surface was examined, and the effects of EPS of different growth

phases on the adhesive and mechanical properties of whole cells were investigated. EPS of the stationary phase are capable of storing more charge than EPS of the exponential phase in the corresponding electric double layer. It is concluded that EPS of the stationary growth stage contribute significantly to cell–mineral interactions than those of the exponential stage. During the retraction of the cell probe from the model silicon oxide surface, more adhesive interactions were found between rhodococcal cells of the stationary phase and the substrate, which were attributed to the chemical composition of the EPS. Due to the nature of weak polyelectrolytes, the conformation of EPS chains is easily affected by the condition of the surrounding medium. The magnitude of the adhesion between EPS and a silicon oxide surface is affected by pH since the density of the available binding sites changes by contracting and stretching the EPS of the stationary phase. The cell spring constant calibration shows that both EPS could confine water. However, successive compressions in an environment where EPS chains are fully stretched show that EPS of the exponential phase cannot resist compression and water can easily be forced away; EPS of the stationary phase is more resilient to compression so as to retain water.

### Acknowledgements

YP thanks Dr Dayi Zhang for the helpful discussions about planktonic cells and EPS; Dr Nicolas Mullin for demonstrating AFM Tapping Mode imaging; and Dr Achim Schmalenberger, Mr Bennett Nwaobi, and Mr Abubakar Elayatt for demonstrating *Rhodococcus* cultivation. ALMG thanks Dr Dayi Zhang for providing the LB medium and Dr Rachel Walton, Alexander McFarlane, and Dr Stephen Rolfe for their help with the fluorescence studies. Funding from the Engineering and Physical Sciences Research Council (GR/S74267/01 and EP/I012060/1) is acknowledged.

### Appendix A. Supplementary data

Supplementary data to this article can be found online at <http://dx.doi.org/10.1016/j.bbamem.2014.11.007>.

### References

- [1] M. Alexander, Biodegradation and Bioremediation, 2nd ed. Academic Press, San Diego, 1999.
- [2] N.A. Sorkhoh, M.A. Ghannoum, A.S. Ibrahim, R.J. Stretton, S.S. Radwan, Crude oil and hydrocarbon-degrading strains of *Rhodococcus rhodochrous* isolated from soil and marine environments in Kuwait, *Environ. Pollut.* 65 (1990) 1–17.
- [3] A.K. Bej, D. Saul, J. Aislabie, Cold-tolerant alkane-degrading *Rhodococcus* species from Antarctica, *Polar Biol.* 23 (2000) 100–105.
- [4] D. Dean-Ross, J.D. Moody, J.P. Freeman, D.R. Doerge, C.E. Cerniglia, Metabolism of anthracene by a *Rhodococcus* species, *FEMS Microbiol. Lett.* 204 (2001) 205–211.
- [5] H. Taki, K. Syutsubo, R.G. Mattison, S. Harayama, Identification and characterization of o-xylene-degrading *Rhodococcus* spp. which were dominant species in the remediation of o-xylene-contaminated soils, *Biodegradation* 18 (2007) 17–26.
- [6] I.B. Ivshina, T.A. Peshkur, V.P. Korobov, Efficient uptake of cesium ions by *Rhodococcus* cells, *Microbiology* 71 (2002) 357–361.
- [7] W.R. Finnerty, The biology and genetics of the genus *Rhodococcus*, *Annu. Rev. Microbiol.* 46 (1992) 193–218.
- [8] S.A. Denome, E.S. Olson, K.D. Young, Identification and cloning of genes involved in specific desulfurization of dibenzothiophene by *Rhodococcus* sp. strain IGTS8, *Appl. Environ. Microbiol.* 59 (1993) 2837–2843.
- [9] J.L.M. Rodrigues, C.A. Kachel, M.R. Aiello, J.F. Quensen, O.V. Maltseva, T.V. Tsoi, J.M. Tiedje, Degradation of Aroclor 1242 dechlorination products in sediments by *Burkholderia xenovorans* LB400(ohb) and *Rhodococcus* sp. strain RHA1(fcb), *Appl. Environ. Microbiol.* 72 (2006) 2476–2482.
- [10] H. Aoshima, T. Hirase, T. Tada, N. Ichimura, H. Kato, Y. Nagata, T. Myoenzono, M. Taguchi, K. Takahashi, T. Hukuzumi, T. Aoki, S. Makino, K. Hagiya, H. Ishiwata, Safety evaluation of a heavy oil-degrading bacterium, *Rhodococcus erythropolis* C2, *J. Toxicol. Sci.* 32 (2007) 69–78.
- [11] D. Kitamoto, H. Isoda, T. Nakahara, Functions and potential applications of glycolipid biosurfactants: from energy-saving materials to gene delivery carriers, *J. Biosci. Bioeng.* 94 (2002) 187–201.
- [12] M.S. Kuyukina, I.B. Ivshina, S.V. Gein, T.A. Baeva, V.A. Chereshev, *In vitro* immunomodulating activity of biosurfactant glycolipid complex from *Rhodococcus ruber*, *Bull. Exp. Biol. Med.* 144 (2007) 326–330.
- [13] S. Lang, J.C. Philp, Surface-active lipids in *Rhodococci*, A. Van. Leeuw, *J. Microb.* 74 (1998) 59–70.
- [14] T.R. Neu, J.R. Lawrence, In situ characterization of extracellular polymeric substances (EPS) in biofilm systems, in: J. Wingender, T.R. Neu, H.C. Flemming (Eds.), *Microbial Extracellular Polymeric Substances: Characterization, Structure and Function*, Springer, Berlin, 1999.
- [15] A.W. Decho, G.R. Lopez, Exopolymer microenvironments of microbial flora: multiple and interactive effects on trophic relationships, *Limnol. Oceanogr.* 38 (1993) 1633–1645.
- [16] M. Hoffman, A.W. Decho, Extracellular enzymes within microbial biofilms and the role of the extracellular polymer matrix, in: J. Wingender, T.R. Neu, H.C. Flemming (Eds.), *Microbial Extracellular Polymeric Substances: Characterization, Structure and Function*, Springer, Berlin, 1999.
- [17] W.B. Dade, J.D. Davis, P.D. Nichols, A.R.M. Nowell, D. Thistle, M.B. Trexler, D.C. White, Effects of bacterial exopolymer adhesion on the entrainment of sand, *Geomicrobiol. J.* 8 (1990) 1–16.
- [18] M. Geoghegan, J.S. Andrews, C.A. Biggs, K.E. Eboigbodin, D.R. Elliott, S. Rolfe, J. Scholes, J.J. Ojeda, M.E. Romero-Gonzalez, R.G.J. Edyvean, L. Swanson, R. Rutkate, R. Fernando, Y. Pen, Z. Zhang, S.A. Banwart, The polymer physics and chemistry of microbial cell attachment and adhesion, *Faraday Discuss.* 139 (2008) 85–103.
- [19] J.J. Ojeda, M.E. Romero-González, R.T. Bachmann, R.G.J. Edyvean, S.A. Banwart, Characterization of the cell surface and cell wall chemistry of drinking water bacteria by combining XPS, FTIR spectroscopy, modeling, and potentiometric titrations, *Langmuir* 24 (2008) 4032–4040.
- [20] Z. Zhang, Y. Pen, R.G. Edyvean, S.A. Banwart, R.M. Dalglish, M. Geoghegan, Adhesive and conformational behaviour of mycolic acid monolayers, *BBA Biomembr.* 1798 (2010) 1829–1839.
- [21] K. Kato, E. Uchida, E.-T. Kang, Y. Uyama, Y. Ikada, Polymer surface with graft chains, *Prog. Polym. Sci.* 28 (2003) 209–259.
- [22] E.P.K. Currie, W. Norde, M.A.C. Stuart, Tethered polymer chains: surface chemistry and their impact on colloidal and surface properties, *Adv. Colloid Interf. Sci.* 100–102 (2003) 205–265.
- [23] R.F. Conside, C.J. Drummond, D.R. Dixon, Force of interaction between a biocolloid and an inorganic oxide: complexity of surface deformation, roughness, and brushlike behavior, *Langmuir* 17 (2001) 6325–6335.
- [24] T.A. Camesano, B.E. Logan, Probing bacterial electrostatic interactions using atomic force microscopy, *Environ. Sci. Technol.* 34 (2000) 3354–3362.
- [25] F. Gaboriaud, Y.F. Dufrene, Atomic force microscopy of microbial cells: application to nanomechanical properties, surface forces and molecular recognition forces, *Colloids Surf. B* 54 (2007) 10–19.
- [26] H.C. Flemming, J. Wingender, The biofilm matrix, *Nat. Rev. Microbiol.* 8 (2010) 623–633.
- [27] F. Oosawa, *Polyelectrolytes*, 1st ed. Marcel Dekker, New York, 1971.
- [28] H.J. Butt, M. Kappl, Surface forces in polymer solutions and melts, *Surface and Interfacial Forces*, Wiley-VCH, Weinheim, 2010.
- [29] G. Hadziioannou, S. Patel, S. Granick, M. Tirrell, Forces between surfaces of block copolymers adsorbed on mica, *J. Am. Chem. Soc.* 108 (1986) 2869–2876.
- [30] S. Hayashi, T. Abe, N. Higashi, M. Niwa, K. Kurihara, Polyelectrolyte brush layers studied by surface forces measurement: dependence on pH and salt concentrations and scaling, *Langmuir* 18 (2002) 3932–3944.
- [31] S. Block, C.A. Helm, Measurement of long-ranged steric forces between polyelectrolyte layers physisorbed from 1 M NaCl, *Phys. Rev. E* 76 (2007) 030801.
- [32] S. Biggs, Steric and bridging forces between surfaces bearing adsorbed polymer: an atomic force microscopy study, *Langmuir* 11 (1995) 156–162.
- [33] A. Jahn, P.H. Nielsen, Extraction of extracellular polymeric substances (EPS) from biofilms using a cation exchange resin, *Water Sci. Technol.* 32 (1995) 157–164.
- [34] M.F. Dignac, V. Urbain, D. Rybacki, A. Bruchet, D. Snidaro, P. Scribe, Chemical description of extracellular polymers: implication on activated sludge floc structure, *Water Sci. Technol.* 38 (1998) 45–53.
- [35] B.P. Frank, G. Belfort, Intermolecular forces between extracellular polysaccharides measured using the atomic force microscope, *Langmuir* 13 (1997) 6234–6240.
- [36] G.A. Burks, S.B. Velegol, E. Paramonova, B.E. Lindenmuth, J.D. Feick, B.E. Logan, Macroscopic and nanoscale measurements of the adhesion of bacteria with varying outer layer surface composition, *Langmuir* 19 (2003) 2366–2371.
- [37] V. Vadillo-Rodríguez, J.R. Dutcher, Viscoelasticity of the bacterial cell envelope, *Soft Matter* 7 (2011) 4101–4110.
- [38] E.S. Taylor, S.K. Lower, Thickness and surface density of extracellular polymers on *Acidithiobacillus ferrooxidans*, *Appl. Environ. Microbiol.* 74 (2008) 309–311.
- [39] N.I. Abu-Lail, T.A. Camesano, The effect of solvent polarity on the molecular surface properties and adhesion on *Escherichia coli*, *Colloids Surf. B* 51 (2006) 62–70.
- [40] J. Strauss, N.A. Burnham, T.A. Camesano, Atomic force microscopy study of the role of LPS O-antigen on adhesion of *E. coli*, *J. Mol. Recognit.* 22 (2009) 347–355.
- [41] H.J. Butt, B. Cappella, M. Kappl, Force measurements with the atomic force microscope: technique, interpretation and applications, *Surf. Sci. Rep.* 59 (2005) 1–152.
- [42] J.S. Andrews, S.A. Rolfe, W.E. Huang, J.D. Scholes, S.A. Banwart, Biofilm formation in environmental bacteria is influenced by different macromolecules depending on genus and species, *Environ. Microbiol.* 12 (2010) 2496–2507.
- [43] G. Fleminger, Y. Shabtai, Direct and rapid analysis of the adhesion of bacteria to solid surface: interaction of fluorescently labeled *Rhodococcus* strain GIN-1 (NCIMB 40340) cells with titanium-rich particles, *Appl. Environ. Microbiol.* 61 (1995) 4357–4361.
- [44] M. Kobayashi, N. Yanaka, T. Nagasawa, H. Yamada, Purification and characterization of a novel nitrilase of *Rhodococcus rhodochrous* K22 that acts on aliphatic nitriles, *J. Bacteriol.* 172 (1990) 4807–4815.
- [45] R.S. Pembrey, K.C. Marshall, R.P. Schneider, Cell surface analysis techniques: what do cell preparation protocols do to cell surface properties? *Appl. Environ. Microbiol.* 65 (1999) 2877–2894.

- [46] K.E. Bremmell, A. Evans, C.A. Prestidge, Deformation and nano-rheology of red blood cells: an AFM investigation, *Colloids Surf. B* 50 (2006) 43–48.
- [47] V.J. Morris, A.R. Kirby, A.P. Gunning, *Atomic Force Microscopy for Biologists*, 2nd ed. Imperial College Press, London, 2010.
- [48] S.K. Lower, C.J. Tadanier, M.F. Hochella, Measuring interfacial and adhesion forces between bacteria and mineral surfaces with biological force microscopy, *Geochim. Cosmochim. Acta* 64 (2000) 3133–3139.
- [49] S.K. Lower, M.F. Hochella Jr., T.J. Beveridge, Bacterial recognition of mineral surfaces: nanoscale interactions between *Shewanella* and  $\alpha$ -FeOOH, *Science* 292 (2001) 1360–1363.
- [50] J.L. Hutter, J. Bechhoefer, Calibration of atomic force microscope tips, *Rev. Sci. Instrum.* 64 (1993) 1868–1873.
- [51] R.F. Considine, D.R. Dixon, C.J. Drummond, Laterally-resolved force microscopy of biological microspheres-ocysts of *Cryptosporidium parvum*, *Langmuir* 16 (2000) 1323–1330.
- [52] H.C. van der Mei, H.J. Busscher, R. Bos, J. de Vries, C.J.P. Boonaert, Y.F. Dufrêne, Direct probing by atomic force microscopy of the cell surface softness of a fibrillated and nonfibrillated oral streptococcal strain, *Biophys. J.* 78 (2000) 2668–2674.
- [53] V. Vadillo-Rodríguez, H.J. Busscher, W. Norde, J. de Vries, H.C. van der Mei, On relations between microscopic and macroscopic physicochemical properties of bacterial cell surfaces: an AFM study on *Streptococcus mitis* strains, *Langmuir* 19 (2003) 2372–2377.
- [54] W.A. Ducker, Z. Xu, J.N. Israelachvili, Measurements of hydrophobic and DLVO forces in bubble-surface interactions in aqueous solutions, *Langmuir* 10 (1994) 3279–3289.
- [55] P. Pincus, Colloid stabilization with grafted polyelectrolytes, *Macromolecules* 24 (1991) 2912–2919.
- [56] J. Rühe, M. Ballauff, M. Biesalski, P. Dziezok, F. Grohn, D. Johannsmann, N. Houbenov, N. Hugenberg, R. Konradi, S. Minko, M. Motornov, R.R. Netz, M. Schmidt, C. Seidel, M. Stamm, T. Stephan, D. Usov, H.N. Zhang, Polyelectrolyte brushes, in: M. Schmidt (Ed.), *Polyelectrolytes with Defined Molecular Architecture I*, Springer, Berlin, 2004.
- [57] H.J. Butt, M. Kappl, *Surface and Interfacial Forces*, 1st ed. Wiley-VCH, Weinheim, 2010.
- [58] F. Ahimou, F.A. Denis, A. Touhami, Y.F. Dufrêne, Probing microbial cell surface charges by atomic force microscopy, *Langmuir* 18 (2002) 9937–9941.
- [59] T.A. Camesano, Y.T. Liu, M. Datta, Measuring bacterial adhesion at environmental interfaces with single-cell and single-molecule techniques, *Adv. Water Resour.* 30 (2007) 1470–1491.
- [60] J. Nigou, M. Gilleron, G. Puzo, Lipoarabinomannans: from structure to biosynthesis, *Biochimie* 85 (2003) 153–166.
- [61] M. Gilleron, N.J. Garton, J. Nigou, T. Brando, G. Puzo, I.C. Sutcliffe, Characterization of a truncated lipoarabinomannan from the Actinomycete *Turicella otitidis*, *J. Bacteriol.* 187 (2005) 854–861.
- [62] J. Nigou, T. Vasselon, A. Ray, P. Constant, M. Gilleron, G.S. Besra, I. Sutcliffe, G. Tiraby, G. Puzo, Mannan chain length controls lipoglycans signaling via and binding to TLR2, *J. Immunol.* 180 (2008) 6696–6702.
- [63] I.C. Sutcliffe, A.K. Brown, L.G. Dover, The Rhodococcal cell envelope: composition, organisation and biosynthesis, in: H.M. Alvarez (Ed.), *Biology of Rhodococcus*, Springer, Heidelberg, 2010.
- [64] S.W. Hunter, H. Gaylord, P.J. Brennan, Structure and antigenicity of the phosphorylated lipopolysaccharide antigens from the Leprosy and *Tubercle bacilli*, *J. Biol. Chem.* 261 (1986) 12345–12351.
- [65] B. Bendinger, H.H.M. Rijnaarts, K. Altendorf, A.J.B. Zehnder, Physicochemical cell-surface and adhesive properties of coryneform bacteria related to the presence and chain-length of mycolic acids, *Appl. Environ. Microbiol.* 59 (1993) 3973–3977.
- [66] M.J. Vacheron, M. Guinand, G. Michel, J.M. Ghuysen, Structural investigations on cell walls of *Nocardia* sp.: the wall lipid and peptidoglycan moieties of *Nocardia kirovani*, *Eur. J. Biochem.* 29 (1972) 156–166.
- [67] M. Arnoldi, M. Fritz, E. Bäuerlein, M. Radmacher, E. Sackmann, A. Boulbitch, Bacterial turgor pressure can be measured by atomic force microscopy, *Phys. Rev. E* 62 (2000) 1034–1044.
- [68] M. Arnoldi, C.M. Kacher, E. Bäuerlein, M. Radmacher, M. Fritz, Elastic properties of the cell wall of *Magnetospirillum gryphiswaldense* investigated by atomic force microscopy, *Appl. Phys. A Mater.* 66 (1998) S613–S617.
- [69] X. Yao, J. Walter, S. Burke, S. Stewart, M.H. Jericho, D. Pink, R. Hunter, T.J. Beveridge, Atomic force microscopy and theoretical considerations of surface properties and turgor pressures of bacteria, *Colloids Surf. B* 23 (2002) 213–230.
- [70] M. Geoghegan, L. Ruiz-Pérez, C.C. Dang, A.J. Parnell, S.J. Martin, J.R. Howse, R.A.L. Jones, R. Golestanian, P.D. Topham, C.J. Crook, A.J. Ryan, D.S. Sivia, J.R.P. Webster, A. Menelle, The pH-induced swelling and collapse of a polybase brush synthesized by atom transfer radical polymerization, *Soft Matter* 2 (2006) 1076–1080.
- [71] S. Rauch, P. Uhlmann, K.-J. Eichhorn, In situ spectroscopic ellipsometry of pH-responsive polymer brushes on gold substrates, *Anal. Bioanal. Chem.* 405 (2013) 9061–9069.
- [72] T.R. Neu, T. Dengler, B. Jann, K. Poralla, Structural studies of an emulsion-stabilizing exopolysaccharide produced by an adhesive, hydrophobic *Rhodococcus* strain, *J. Gen. Microbiol.* 138 (1992) 2531–2537.
- [73] I.W. Sutherland, Microbial exopolysaccharides-structural subtleties and their consequences, *Pure Appl. Chem.* 69 (1997) 1911–1917.
- [74] A.F. Kennedy, I.W. Sutherland, Analysis of bacterial exopolysaccharides, *Biotechnol. Appl. Biochem.* 9 (1987) 12–19.
- [75] T.R. Neu, Significance of bacterial surface-active compounds in interaction of bacteria with interfaces, *Microbiol. Rev.* 60 (1996) 151–166.
- [76] L.M. Mayer, L.L. Schick, T. Sawyer, C.J. Plante, P.A. Jumars, R.L. Self, Bioavailable amino acids in sediments: a biomimetic, kinetics-based approach, *Limnol. Oceanogr.* 40 (1995) 511–520.
- [77] P.E. Kepkay, Particle aggregation and the biological reactivity of colloids, *Mar. Ecol. Prog. Ser.* 109 (1994) 293–304.
- [78] D.G. Allison, I.W. Sutherland, The role of exopolysaccharides in adhesion of freshwater bacteria, *J. Gen. Microbiol.* 133 (1987) 1319–1327.